European Journal of Medicinal Chemistry 221 (2021) 113524

Contents lists available at ScienceDirect

European Journal of Medicinal Chemistry

journal homepage: http://www.elsevier.com/locate/ejmech

Lanosterol 14α-demethylase (CYP51)/histone deacetylase (HDAC) dual inhibitors for treatment of *Candida tropicalis* and *Cryptococcus neoformans* infections

Tianbao Zhu [a, b, 1], Xi Chen [c, 1], Chenglan Li [b], Jie Tu [b], Na Liu [b, ***], Defeng Xu [a, **], Chunquan Sheng [b, *]

[a] National & Local Joint Engineering Research Center for High-efficiency Refining and High-quality Utilization of Biomass, School of Pharmacy, 1 Gehu Road, Changzhou University, Changzhou, 213164, China
[b] School of Pharmacy, Second Military Medical University, 325 Guohe Road, Shanghai, 200433, China
[c] Key Laboratory of Synthetic and Natural Functional Molecule of the Ministry of Education, College of Chemistry and Materials Science, Northwest University, 1 Xuefu Avenue, Xi'an, 710127, China

ARTICLE INFO

Article history:
Received 7 December 2020
Received in revised form
28 April 2021
Accepted 30 April 2021
Available online 7 May 2021

Keywords:
Antifungal
CYP51/HDAC dual Inhibitors
Virulence factors
Cryptococcus neoformans
Candida tropicalis

ABSTRACT

Invasive fungal infections remain a challenge due to lack of effective antifungal agents and serious drug resistance. Discovery of antifungal agents with novel antifungal mechanism is important and urgent. Previously, we designed the first CYP51/HDAC dual inhibitors with potent activity against resistant *Candida albicans* infections. To better understand the antifungal spectrum and synergistic mechanism, herein new CYP51/HDAC dual inhibitors were designed which showed potent *in vitro* and *in vivo* antifungal activity against *C. neoformans* and *C. tropicalis* infections. Antifungal mechanism studies revealed that the CYP51/HDAC dual inhibitors acted by inhibiting various virulence factors of *C. tropicalis* and *C. neoformans* and down-regulating resistance-associated genes. This study highlights the potential of CYP51/HDAC dual inhibitors as a promising strategy for the discovery of novel broad-spectrum antifungal agents.

1. Introduction

In recent years, the morbidity and mortality of invasive fungal infections (IFIs) are continuing to increase due the large population of immunocompromised patients suffering from tumor, organ transplantation, acquired immune deficiency syndrome (AIDS) and so on [1,2]. *Candida, Cryptococcus and Aspergillus* are the major pathogens in clinical IFIs. Among the *Candida* spp., *Candida tropicalis* (*C. tropicalis*), accounting for 45% of non-*Candida albicans* infections, has become the second common species of *Candida* bloodstream infection [3,4]. *Cryptococcus neoformans* (*C. neoformans*) is one of the most common fungi species with high mortality rate [5,6]. Particularly, the incidence of cryptococcal meningitis (CM) caused by *C. neoformans* frequently occurred in AIDS patients with the mortality rate over 15% [7]. In addition, it is estimated that more than 22 thousand individuals suffer from CM annually [8]. Traditional antifungal drugs used to treat IFIs include: polyenes, pyrimidines, azoles and echinocandins [9,10]. However, due to severe drug resistance and side effects of clinically available antifungal drugs, therapeutic effect of IFIs remains rather limited. Therefore, there is an urgent need for the development of mechanistically distinct antifungal agents.

Histone acetylation modification, including histone acetylation and deacetylation, is an important component of epigenetic research. As a series of enzymes with deacetylation function, histone deacetylases (HDACs) account for an important role in the

* Corresponding author.
** Corresponding author.
*** Corresponding author.
E-mail addresses: liuna@smmu.edu.cn (N. Liu), markxu@cczu.edu.cn (D. Xu), shengcq@smmu.edu.cn (C. Sheng).
[1] These authors contributed equally to this work.

https://doi.org/10.1016/j.ejmech.2021.113524
0223-5234/

chromosomes remodeling and regulation of gene expression [11,12]. HDACs in fungi, such as *Aspergillus fumigatus* [13], *Candida albicans* [14,15], *Saccharomyces cerevisiae* [16], and *C. neoformans* HDACs [17,18] have been reported to participate in virulence-related processes and morphological changes. Therefore, inhibition of fungal HDACs could be an effective strategy to treat fungal infections. Recently, HDAC inhibitors have been proven to be synergized with azole antifungal drugs [19,20]. For example, HDAC inhibitor MGCD290 synergized with fluconazole (FLC) against a variety of clinical fungal isolates [21]. In addition, HDAC inhibitors trichostatin A (TSA) and vorinostat (SAHA) synergized with itraconazole (ICA) and FLC against azole-resistant *Candida albicans* (*C. albicans)* and *C. tropicalis* [22,23]. However, the synergistic mechanism and *in vivo* antifungal activity of azoles synergized with HDAC inhibitors are still unclear.

Clinically, specific drug combination is important for disease control, whereas drug cocktails have the disadvantages of drug-drug interaction, poor patient compliance and unpredictable pharmacokinetic (PK) profiles [24]. Therefore, multi-targeting drug is a feasible solution to retain the synergistic effect and overcome these limitations. Previously, JAK/HDAC dual inhibitors were designed by our group, which exhibited excellent synergistic antifungal potency for the treatment of acute myeloid leukemia (AML) and azole-resistant *C. albicans* infection [25]. In addition, we also designed the first generation of lanosterol 14α-demethylase (CYP51)/HDAC dual inhibitors, which exhibited excellent *in vitro* and *in vivo* antifungal activity against azole-resistant *C. albicans* infections [26]. These proof-of-concept studies offered a promising way for the treatment of resistant fungal infections. However, it is still unknown that whether the CYP51/HDAC dual inhibitors are effective in treating non-*C. albicans* infections. In an attempt to further investigate the antifungal spectrum and synergistic mechanism, herein new CYP51/HDAC dual inhibitors were designed (Fig. 1). After *in vitro* and *in vivo* investigation of the antifungal activity and mechanism, the dual inhibitors showed potent antifungal activity against *C. neoformans* and azole-resistant *C. tropicalis* infections by inhibiting virulence factors and down-regulating resistance-associated genes.

2. Results and discussion

2.1. Introducing piperazine substituents to design CYP51/HDAC dual inhibitors

Previously, we reported the first example of CYP51/HDAC dual inhibitors [26]. It represents a novel strategy for the treatment of azole-resistant Candidiasis. Herein, for further investigating the structure-activity relationship (SAR) of CYP51/HDAC dual inhibitors and developing more efficient broad-spectrum antifungal compounds, a new series of CYP51/HDAC dual inhibitors containing the piperazine linker were designed by the key pharmacophore fusion of CYP51 and HDAC inhibitors. In general, HDAC inhibitors contain a cap group, a variable linker and a zinc-binding group (ZBG). ZBG (*e.g.* hydroxamic acid) is critical for the inhibition of zinc-dependent HDACs, while diverse skeletons can be used as the cap group (Fig. 1A). The key pharmacophores of typical azoles include a triazole group, a 2,4-difluorophenyl group and a variable side chain (Fig. 1B). On the basis of the pharmacophores and binding modes [26], CYP51/HDAC dual inhibitors can be designed by the fusion of triazole, 2,4-difluorophenyl group and ZBG. In our previous study, side chains of the first generation CYP51/HDAC dual inhibitors are mainly flexible structures. Herein, piperazine group was introduced as a part of linker to increase structural rigidity and adjust the physicochemical properties (Fig. 1C). Consequently, four types CYP51/HDAC dual inhibitors with different linkers were designed: alkoxybenzyl linker (benzene ring is linked to piperazine by methylene, **A1-A5**), phenylalkoxyl linker (alkoxy is linked to piperazine, **A6-A8**), 1,3-diphenoxypropane (**A9**), and triazolone alkoxybenzyl (**A10-A13**, Fig. 1D).

2.2. Chemistry

The synthesis routes of target compounds **A1-A13** are described in Schemes 1–4. Starting materials **1**, **2a-2e**, **4**, **9**, **10a-10c** are commercially available. Intermediate oxirane **7** was synthesized according to the reported methods [27]. Treating brominated compounds **2a-2e** with hydroxybenzaldehyde **1** in K_2CO_3 and

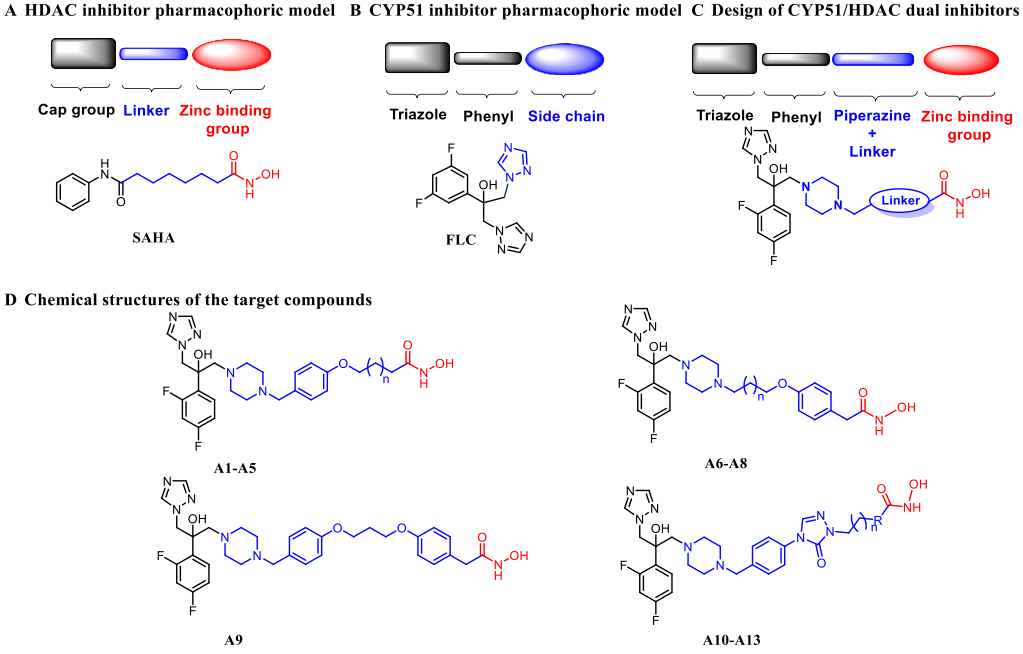

Fig. 1. Design strategies of CYP51/HDAC dual inhibitors. (A) Pharmacophoric model of HDAC inhibitors; (B) pharmacophoric model of CYP51 inhibitors; (C) Design of CYP51/HDAC dual inhibitors; (D) Chemical structures of the target compounds.

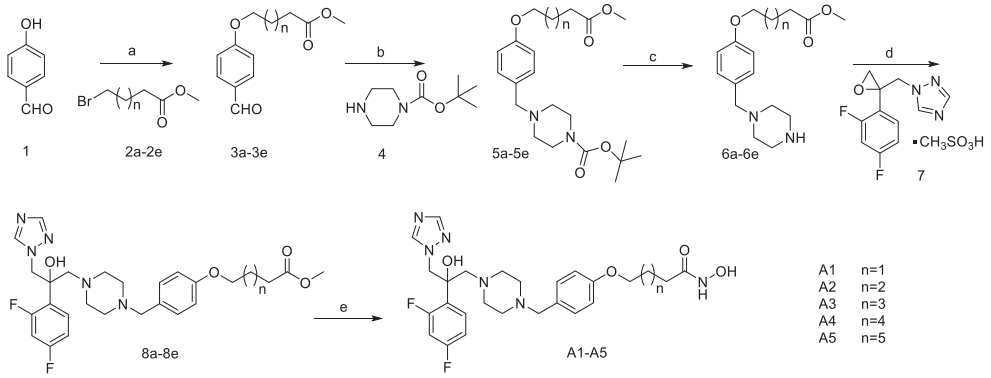

Scheme 1. [a] Reagents and conditions: (a) EtOH, K_2CO_3, 85 °C, reflux, 5 h; (b) (i) Ti(*i*-propoxyl)$_4$, Et_3N, MeOH, rt, 12 h, (ii) $NaBH_4$, rt, 30 min; (c) TFA, CH_2Cl_2, rt, 1 h; (d) K_2CO_3, anhydrous DMF, 85 °C, 12 h; (e) NH_2OH HCl, KOH, MeOH, rt, 5 h.

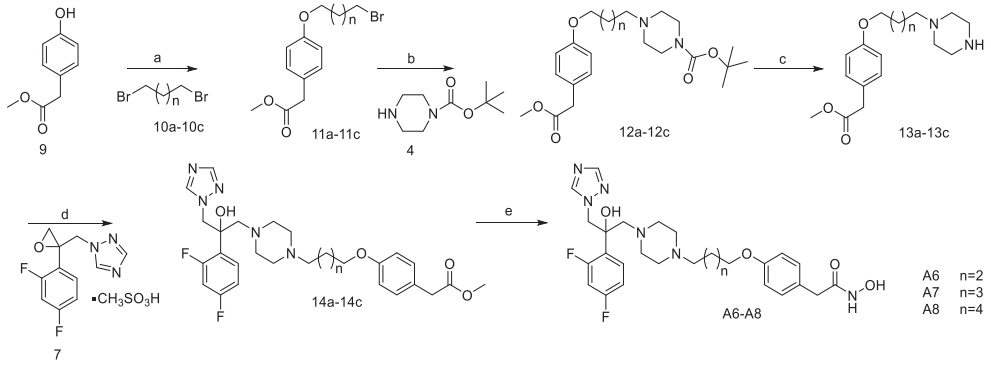

Scheme 2. [a] Reagents and conditions: (a) (b) K_2CO_3, EtOH, 85 °C, 12 h; (c) TFA, CH_2Cl_2, rt, 1 h; (d) K_2CO_3, anhydrous DMF, 85 °C, 12 h; (e) NH_2OH HCl, KOH, MeOH, rt, 5 h.

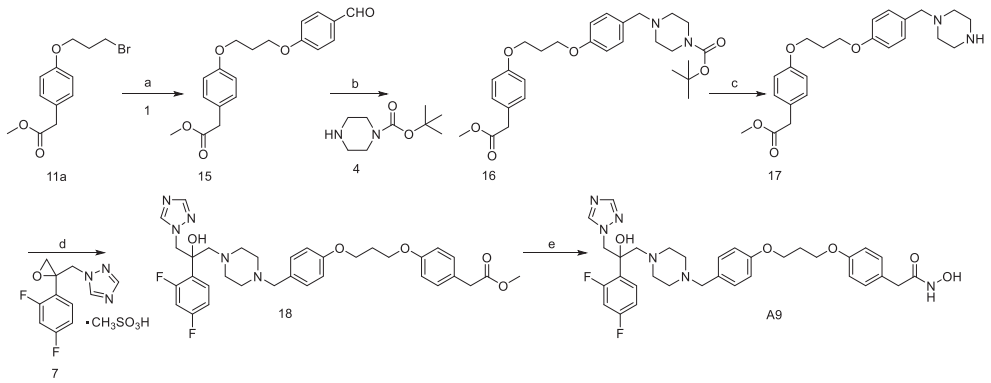

Scheme 3. [a] Reagents and conditions: (a) K_2CO_3, EtOH, 85 °C, 3 h; (b) (i) Ti(i-propoxyl)$_4$, Et_3N, MeOH, rt, 12 h; (ii) $NaBH_4$, rt, 30 min; (c) TFA, CH_2Cl_2, rt, 1 h; (d) K_2CO_3, anhydrous DMF, 85 °C, 12 h; (e) NH_2OH HCl, KOH, MeOH, rt, 5 h.

anhydrous EtOH to give intermediates **3a-3e**, which further reacted with Boc-protected piperazine **4** to afford intermediates **5a-5e**. Then, Boc-protecting group was removed by trifluoroacetic acid (TFA) to afford intermediates **6a-6e**, which further reacted with oxirane **7** to give intermediates **8a-8e**. Finally, intermediates **8a-8e** were reacted with freshly prepared NH_2OH in CH_3OH to obtain target compounds **A1-A5** (Scheme 1).

Target compounds **A6-A8** were synthesized by the route outlined in Scheme 2. Substituted phenol **9** reacted with dibromo-substituted alkanes **10a-10c** to give intermediates **11a-11c**, which further reacted with Boc-protected piperazine **4** via Borch reduction to afford intermediates **12a-12c**. Then, the Boc-protecting group of intermediates **12a-12c** in TFA afforded intermediates **13a-13c**, which reacted with oxirane **7** to form intermediates **14a-14c**. After treating with fresh hydroxylamine, target compounds **A6-A8** were obtained (Scheme 2).

Intermediates **11a** reacted with starting material **1** in the presence of K_2CO_3 and ethanol to give intermediate **15**. By a similar procedure depicted in Scheme 2, intermediate **18** was prepared from intermediate **15** via Borch reduction, deprotection and ring opening, which treating with fresh hydroxylamine to give target compound **A9** (Scheme 3).

Starting material **19** reacted with Boc-protected piperazine **4** by Borch reduction to give intermediate **20**, then nitro group was

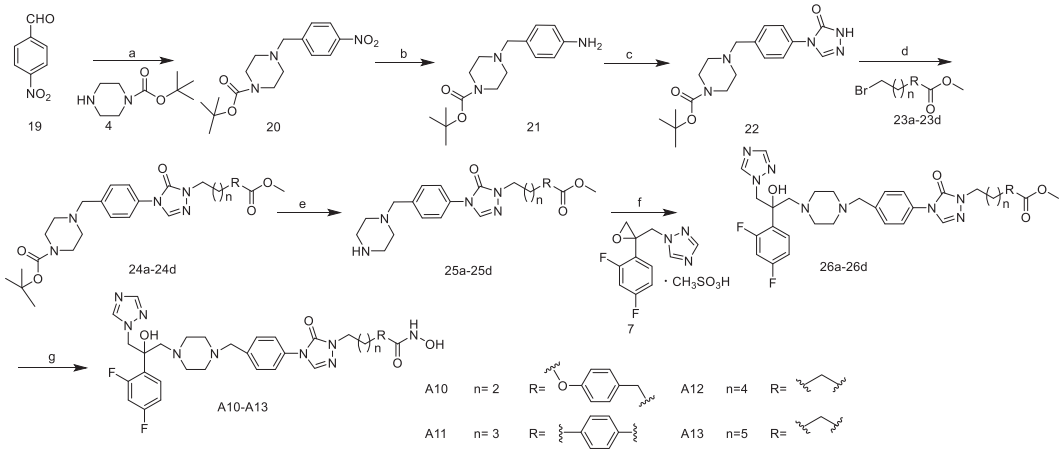

Scheme 4. [a]Reagents and conditions:(a) Ti(*i*-propoxyl)$_4$, Et_3N, MeOH, rt, 12 h; (b) 95% EtOH, Fe, NH_4Cl, reflux, 3 h; (c) methyl hydrazinecarboxylate, trimethoxymethane, MeOH, 70 °C, 6 h; (d) anhydrous DMF, K_2CO_3, 80 °C, 4 h; (e) TFA, CH_2Cl_2, rt, 1 h; (f) K_2CO_3, anhydrous DMF, 85 °C, 12 h; (g) NH_2OH HCl, KOH, MeOH, rt, 5 h.

reduced in the presence of Fe to afford intermediate **21**. Intermediate **21** reacted with hydrazinecarboxylate to give intermediate **22**, which was substituted by brominated compounds **23a-23d** to afford intermediates **24a-24d**. The Boc-protecting groups were removed to give intermediates **25a-25d**. Intermediates **26a-26d** were prepared via ring opening and substitution reaction, and finally treated with fresh hydroxylamine to give target compounds **A10-A13** (Scheme 4).

2.3. In vitro antifungal activity and SAR of CYP51/HDAC dual inhibitors

The antifungal activity of the synthesized CYP51/HDAC dual inhibitors was assayed against *C. neoformans* and azole-resistant *C. tropicalis*, which was expressed by the MIC_{80} value. CYP51 inhibitors FLC, ICA, voriconazole (VRC) and the HDAC inhibitor SAHA were used as positive controls. As shown in Table 1, compounds **A1-A5,** featured as the piperazinylmethylenephenyloxyalkyl linker, showed moderate to good antifungal activity (MIC_{80} range: 0.5 μg/mL ~ 2 μg/mL). The antifungal activity of target compounds **A1**-**A5** was increased with the extension of the alkoxy chains (3—7 carbon atoms). Compound **A5** (7 carbon atoms length) exhibited the best inhibitory activity against both *C. tropicalis* and *C. neoformans* with an MIC_{80} of 0.5 μg/mL. In particular, it showed excellent activity towards azoles resistant *C. tropicalis*, whereas positive controls FLC, VOR, ITR and SAHA were not totally inactive. When the direction of alkoxybenzene was changed (alkoxy is linked to piperazine, **A6-A8**), antifungal activity was decreased obviously. Compound **A9** with the 1,3-diphenoxypropane linker showed moderate antifungal activity (MIC_{80} range: 2 μg/mL ~ 32 μg/mL). Among triazolone derivatives **A10-A13**, only compound **A10** showed obvious activity against both FLC-sensitive *C. tropicalis* and *C. neoformans* with an MIC_{80} of 2 μg/mL, while compounds **A11-A13** lost the antifungal effects.

In addition, the antifungal activity of compound **A1-A13** against *C. albicans* was also investigated. Different from our previously reported CYP51/HDAC dual inhibitors, compound **A1-A13** generally exhibited weak to moderate inhibitory activity against azoles-resistant *C. albicans* with an MIC_{80} value range from 1 μg/mL to 64 μg/mL. The inhibitory effects of compounds **A1-A13** against FLC-sensitive *C. albicans* were also inferior to FLC (Table 2).

Considering the excellent antifungal activity, compound **A5** was selected for further biological activity evaluation and mechanism study. Initially. we investigated the cytotoxicity of compound **A5** against HUVEC (human umbilical vein endothelial cell line) with an IC_{50} value of 5.9 μg/mL (10.36 μM), which was approximately 12 times higher than the MIC_{80} value of 0.5 μg/mL. Preliminary experimental results suggested that compound **A5** had selective antifungal activity with low toxicity to human normal cells.

2.4. Compounds *A5* showed potent inhibitory activities against FLC-resistant C. tropicalis and FLC-sensitive C. neoformans

The time-growth curves assay was performed to further evaluate the efficacy of compound **A5** against *C. tropicalis* and *C. neoformans* cells growth. The results indicated that compound **A5** at 8 μg/mL inhibited the proliferation of *C. tropicalis* cells superior than FLC at a higher concentration of 32 μg/mL (Fig. 2A). In addition, compound **A5** significantly inhibited the growth of *C. neoformans* cells, whose activity was better than FLC (Fig. 2B).

2.5. Compound *A5* inhibited the filamentation of C. tropicalis and the biofilm formation of C. tropicalis and C. neoformans

As a virulence factor of *C. tropicalis*, filamentation plays an important role in pathogenicity and invasiveness [28,29]. Fungal cells in the hyphal phase invade mucosal tissue easily and cause IFIs [30,31]. Moreover, transition between yeast phase and hyphal phase makes fungal cells easier to evade the host recognition or host defense [32,33]. Therefore, the effects of compound **A5** and FLC at different concentrations in inhibiting *C. tropicalis* filamentation were investigated by using the cell inverted imaging microscope. As compared to the control group, compound **A5** effectively inhibited hyphae formation at 1 μg/mL, whereas FLC was poorly active even at 8 μg/mL (Fig. 3A). Fungal biofilm, a high-density structure, prohibits antifungal drugs penetrating into the cells to exert antifungal activity, which is closely related to drug resistance [34—37]. The 2,3-bis-(2-methoxy-4-nitro-5-sulfophenyl)-2*H*-tetrazolium-5-carboxanilide (XTT) reduction method was used to evaluate the effects of compounds **A5** on *C. tropicalis* and *C. neoformans* biofilms with FLC as a positive control. The results indicated that compound **A5** inhibited biofilm formation of *C. tropicalis* and *C. neoformans* in a dose-dependent manner. Especially, compound **A5** showed better activity than FLC against *C. tropicalis*, and disrupted biofilm formation completely at 64 μg/mL (Fig. 3B). Moreover, compound **A5** approximately blocked 70% of biofilm formation in *C. neoformans* at a high concentration of 64 μg/mL, whereas FLC exhibited the same inhibitory effect at a concentration of 8 μg/mL (Fig. 3B). FLC

Table 1
In vitro antifungal activity of compounds **A1-A13** against *C. tropicalis* and *C. neoformans*.

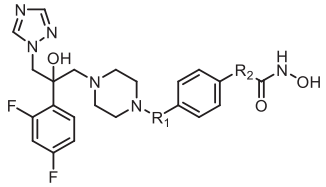

Cpds	R1	R2	*C. tropicalis*		*C. neoformans*
			5008	3890	H99
A1	-CH_2-	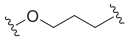	4	4	8
A2	-CH_2-	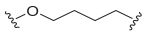	4	2	8
A3	-CH_2-	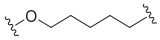	1	2	8
A4	-CH_2-		0.5	2	2
A5	-CH_2-	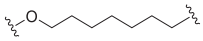	0.5	0.5	0.5
A6	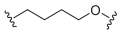	-CH_2-	>64	32	32
A7	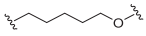	-CH_2-	>64	4	32
A8	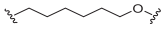	-CH_2-	4	2	16
A9	-CH_2-	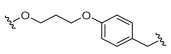	32	2	4
A10	-CH_2-	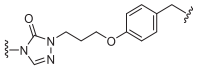	16	2	2
A11	-CH_2-	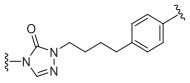	>64	>64	8
A12	-CH_2-	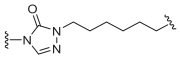	>64	>64	64
A13	-CH_2-	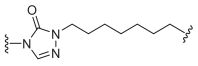	>64	>64	32
FLC	–	–	>64	0.5	2
SAHA	–	–	>64	>64	>64
VOR	–	–	>64	>64	0.0625
ITC	–	–	>64	>64	0.125

Table 2
In vitro antifungal activity of compounds **A1-A13** against *C. albicans*.

Cpds	*C. alb* SC5314	*C. alb.* 0304103	*C. alb.* 7781	*C. alb.* 4108	*C. alb.* 10061	*C. alb.* 9770
A1	4	8	8	16	32	>64
A2	1	8	4	32	>64	>64
A3	1	32	2	16	>64	32
A4	1	16	1	8	32	32
A5	8	8	1	8	16	16
A6	>64	32	>64	>64	>64	>64
A7	32	>64	>64	>64	>64	>64
A8	16	16	4	16	16	16
A9	4	32	4	32	>64	>64
A10	2	2	2	4	32	32
A11	>64	>64	16	>64	>64	>64
A12	>64	>64	32	NT	NT	>64
A13	>64	64	64	NT	NT	>64
FLC	0.5	>64	>64	>64	>64	>64
SAHA	NT	>64	>64	>64	NT	NT
VRC	<0.125	>64	>64	>64	NT	NT
ICZ	0.5	>64	>64	>64	NT	NT

[α]Abbreviations: *C. alb.*, *Candida. albicans*; NT = Not Tested.

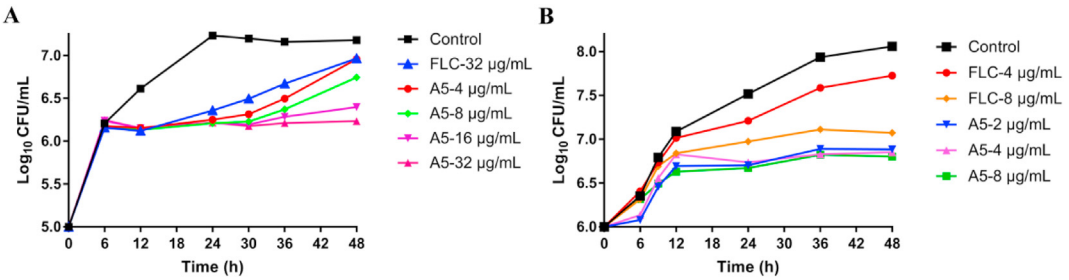

Fig. 2. The time-growth curves of FLC-resistant *C. tropicalis* 5008 cells (A) and FLC-sensitive *C. neoformans* H99 cells (B) treated with the various concentrations compound **A5** as well as FLC at different time periods.

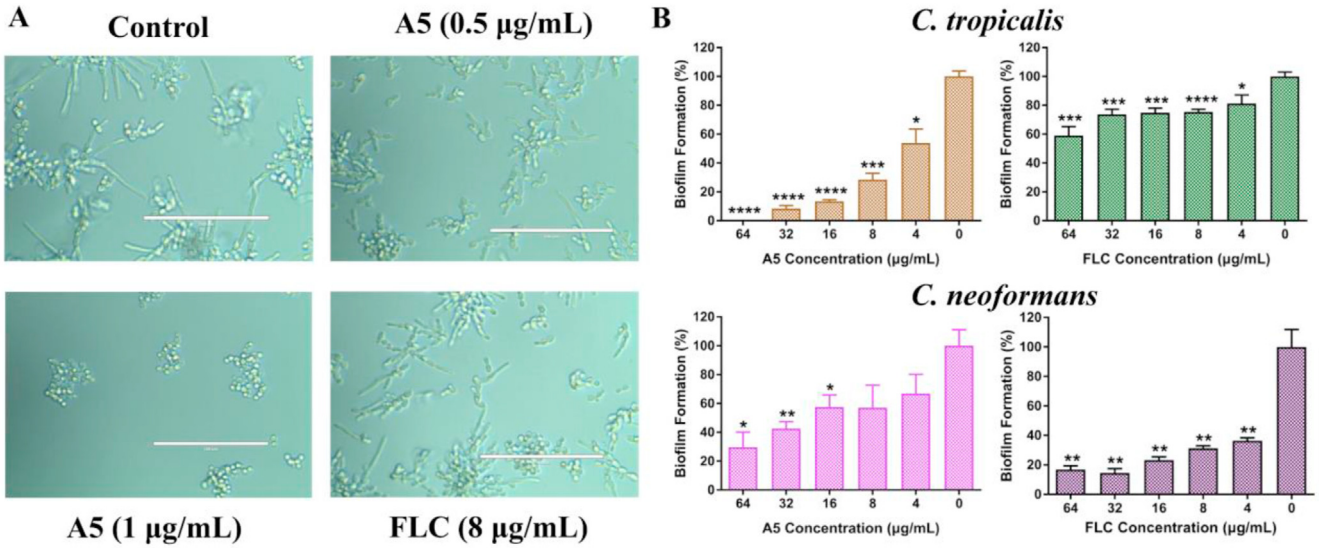

Fig. 3. Inhibitory activity of compound **A5** against filamentation and biofilm formation. (A) The inhibitory effects on the filamentation of *C. tropicalis* 5008 treated with compound **A5** (0.5–1 μg/mL) and FLC (8 μg/mL) at 37 °C for 7 h. (B) The effects of various concentrations of compound **A5** and FLC on the biofilm formation of *C. tropicalis* 5008 and *C. neoformans* H99 compared to no compound treated group. Three independent experiments were conducted and the data was expressed as the mean ± SD. The results were presented as inhibition percentages compared to the untreated groups and the statistical significance was performed by *t*-test (*$P < 0.05$, **$P < 0.01$, ***$P < 0.001$, ****$P < 0.0001$).

performed better at inhibiting the biofilm formation in *C. neoformans* than azole-resistant *C. tropicalis*. Conversely, compound **A5** exhibited better inhibitory effect on azole-resistant *C. tropicalis*.

2.6. Compound **A5** inhibited the formation of *C. neoformans* capsule and down-regulated the capsule-associated genes

As a specific virulence factor of *C. neoformans,* the capsule is a major role in host infection, and protects *C. neoformans* cells from immune attack [38,39]. As show in Fig. 4A and B, the capsule size was reduced significantly after the treatment of compound **A5** ($P < 0.0001$) without inhibitory effects on the growth of the fungi body, whereas the inhibitory effect of FLC with the treatment of equivalent concentration was relatively weak ($P < 0.01$). It is reported that *CAP* genes (*CAP10, CAP59, CAP60, CAP64)* were essential for capsule biosynthesis [38,40]. Therefore, real time RT-PCR was conducted to evaluate the expression levels of four capsule-associated genes after the treatment of compound **A5**. As shown in Fig. 4C, capsule-associated genes *CAP10* and *CAP60* were significantly down-regulated by compound **A5** at 2 μg/mL. In contrast, expression of capsule-associated genes *CAP59* and *CAP64* did not change obviously. When treated with equivalent concentration of FLC, capsule-associated genes *CAP10* and *CAP59* were significantly up-regulated, which led to the weak inhibitory effect on the capsule formation. Thus, compound **A5** could reduce the virulence of *C. neoformans* through down-regulating capsule-associated genes *CAP10* and *CAP60*.

2.7. Analysis of sterol composition and resistance-associated genes

Ergosterol is the main sterol in yeast, which plays an indispensable role in the maintenance of the cell membrane integrity and function [41]. The target of azole antifungal drugs is CYP51, encoded by *ERG11* gene in fungi. The azoles exert antifungal activity by blocking the synthesis of ergosterol and accumulating toxic sterol intermediates [42,43]. Therefore, the influence of compound **A5** on the sterol composition in *C. tropicalis* and *C. neoformans* cell membrane was evaluated by gas chromatography-mass spectrometry (Fig. S1 in Supporting Information). After treated with compound **A5** at a concentration of 4 μg/mL, the ergosterol content of *C. tropicalis* was reduced from 84.91% to 1.51%, with high levels of the obtusifoliol (16.02%) and eburicol (69.34%). As for *C. neoformans*, the ergosterol content was reduced from 60.18% to 19.14% at the same concentration of compound **A5** (Table 3). These results indicated that compound **A5** significantly reduced the fungal ergosterol content by inhibiting CYP51, whose mechanism is similar to that of azole drugs.

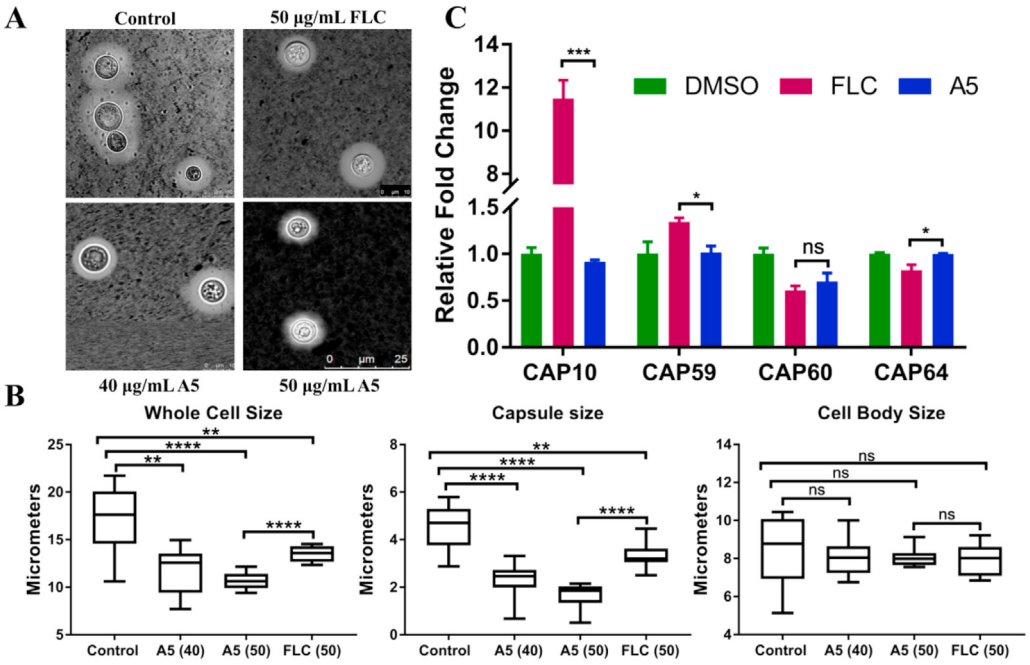

Fig. 4. Effects of compound **A5** on the formation of *C. neoformans* capsule and expression of the capsule-associated genes. (A) The microscopy images of the *C. neoformans* H99 capsule formation were photographed under the high concentrations of compound **A5** or FLC. (B) The data of boxes represent whole cell size, capsule size and cell body size after the treatment of different concentrations of compound **A5** or FLC (measured with imageJ software). (C) Expression levels of four capsule associated-genes in *C. neoformans* H99 with compound **A5** or FLC at a concentration of 2 μg/mL. Three independent experiments of the capsule-associated genes expression were conducted and the data was expressed as the mean ± SD. Statistical significance was performed by *t*-test (**P* < 0.05, ***P* < 0.01, ****P* < 0.001, *****P* < 0.0001).

Table 3
Sterol compositions of FLC-resistant *C. tropicalis* and FLC-sensitive *C. neoformans* after the treatment of compound **A5**.

Sterol	Retention Time (min)	Sterol composition (%)			
		C. tropicalis 5008		*C. neoformans* H99	
		no drug	A5	no drug	A5
Unknown sterol (1)	13.79	5.78	ND	ND	ND
Ergosterol (2)	14.07	84.91	1.51	60.18	19.14
Unknown sterol (3,4)	14.48,14.93	6.48	1.31	ND	ND
Obtusifoliol (5)	15.12	ND	16.02	ND	ND
Lanosterol (6)	15.75	2.81	ND	ND	9.59
Eburicol (7)	16.69	ND	69.34	39.82	71.27

Up to date, azoles resistance have become a serious problem in clinical treatment of IFIs [44]. One major cause is the increased efflux pump proteins (*e.g.* ATP-binding cassette transporters Cdr1p and Mdr1p), which leads to reduced drug concentration in fungal cells [45,46]. Another essential factor of resistance is up-regulation or mutations of the *ERG11* gene in the ergosterol biosynthetic pathway [47]. As shown in Fig. 5, compound **A5** significantly down-regulated the resistant-associated genes (*ERG11, CDR1, MDR1*) in *C. tropicalis* with FLC group as the control. The results indicated that compound **A5** might inhibit the overexpression of efflux pump genes, and down-regulated *ERG11* gene in ergosterol biosynthetic pathway, thus increased the activity against FLC-resistant *C. tropicalis*.

2.8. Compound *A5* inhibited HDAC enzyme activity

According to our previously reported assay with optimized protocols [26], fungal whole cell HDAC enzyme inhibitory activity of compound **A5** was evaluated. Initially, fungal cell wall was lysated to obtain the protoplasts by using snailase. Then HDAC substrate was added after the protoplasts were treated with compound **A5** and SAHA. Finally, inhibitory activity was assessed by monitoring the fluorescence intensity of substrate decomposition. In *C. tropicalis* cells, compound **A5** exhibited stronger HDAC inhibitory activity (IC_{50} = 2.38 μM) than SAHA (IC_{50} = 3.56 μM). However, it was less active in *C. neoformans* cells (Table 4).

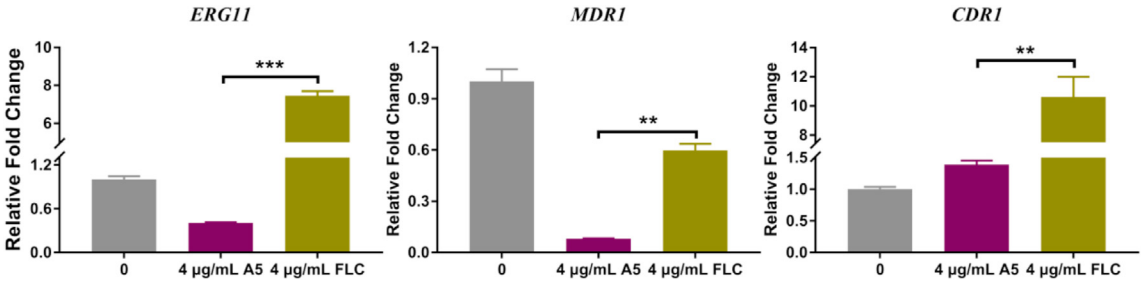

Fig. 5. Different concentrations of compound **A5** stimulated the transcription of the azoles resistant-associated genes *ERG11, CDR1, MDR1* in *C. tropicalis* 5008 with 4 μg/mL FLC as the control. The results are shown by the means ± SD (n = 3 independent assay). ***P* < 0.01, ****P* < 0.001, determined by Student's *t*-test.

2.9. Compound **A5** down-regulated HDAC genes of C. neoformans

Fungal HDACs control cellular processes associated with virulence [48], such as capsule formation, host-pathogen interaction, and melanin synthesis. The "classical" fungal HDAC family proteins of *C. neoformans* divide into two major classes: class I (*e.g.* Rpd3, Hos1, Hos2, Clr61, and Clr62) and class II (Hda1 and Hos3) [48]. Thus, the influence of compound **A5** on the expression of seven HDAC genes of *C. neoformans* was investigated. As shown in Fig. 6, compound **A5** significantly reduced the expression of seven HDAC genes at 2 μg/mL, indicating that down-regulation of HDAC genes by compound **A5** could contribute to reduce pathogenicity of *C. neoformans*.

2.10. In vivo antifungal efficacy of compound **A5**

Due to excellent *in vitro* antifungal activity of compound **A5** against *C. tropicalis* and *C. neoformans*, its *in vivo* antifungal potency was further evaluated in two IFIs mouse models. Mouse models were established by injection with *C. tropicalis* and *C. neoformans* via tail vein with FLC group as positive control. Compound **A5** and FLC were administered orally (20 mg/kg) for 5 consecutive days after 24 h post infection. As shown in Fig. 7A, compared to the saline group, compound **A5** treated group significantly reduced kidney fungal burden of FLC-resistant *C. tropicalis* by about 0.7 log ($P < 0.0001$). In the *C. neoformans* infection model, compound **A5** treated group also effectively reduced brain fungal burden ($P < 0.0001$, Fig. 7B), which was superior to FLC ($P < 0.001$). These results confirmed that compound **A5** exhibited potent therapeutic effects for both tropical candidiasis and CM.

3. Conclusion

In summary, a series of new fungal CYP51/HDAC dual inhibitors were designed and synthesized for the treatment of *C. neoformans* and *C. tropicalis* infections. Among them, compound **A5** showed excellent *in vitro* antifungal activity and significantly reduced fungal burden in two IFIs mouse models. As a CYP51/HDAC dual inhibitor, compound **A5** blocked the biosynthesis of ergosterol and showed potent whole cell HDAC enzyme inhibitory activity. It effectively inhibited important virulence factors (*e.g.* hypha, biofilm and capsule) of *C. neoformans* and *C. tropicalis*, and down-regulated resistance-associated genes. Taken together, this study offered an effective strategy for treatment of CM and FLC-resistant *C. tropicalis* infections.

4. Experimental section

4.1. Chemistry

General Methods. ^{1}H NMR and ^{13}C NMR spectra were recorded on Bruker AVANCE 300, or AVANCE 600 spectrometers (Bruker Company, Germany) using TMS as an internal standard and CD_3OD, $CDCl_3$ or dimethyl sulfoxide (DMSO)-*d6* as solvents. Thin-layer chromatography analysis was performed by using silica gel plates GF254. The chemical purities were analyzed by RP-HPLC with

Table 4
HDAC enzyme inhibition activities (IC_{50}, μM).

Compounds	*C. tropicalis* Whole Cell HDAC	*C. neoformans* Whole Cell HDAC
A5	2.38	12.59
SAHA	3.56	3.11

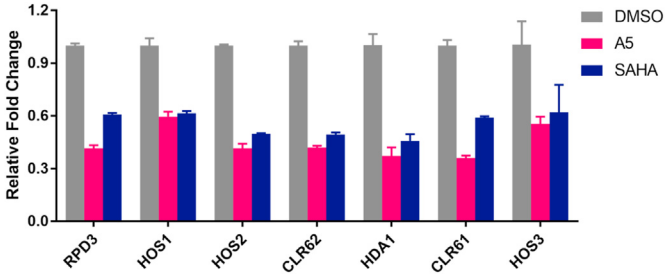

Fig. 6. Expression levels of seven HDAC genes in *C. neoformans* H99 with the treatment of compound **A5** and SAHA at a concentration of 2 μg/mL. The data was shown as means ± SD (n = 3 independent assay).

CH_3OH/H_2O (v/v, 7/3) at a flow rate of 0.5 mL/min on an Agilent C18. The high-resolution mass spectra (HRMS) were recorded on an Agilent UPLC-QTOF/MS mass spectrometer. All final compounds exhibited purities greater than 95%.

4.1.1. 4-(4-((4-(2-(2,4-difluorophenyl)-2-hydroxy-3-(1H-1,2,4-triazol-1-yl)propyl) piper-azin-1-yl)methyl)phenoxy)-N-hydroxybutanamide (**A1**)

The freshly prepared NH_2OH solution in CH_3OH was added into intermediate **8a** (1.77 g, 3.34 mmoL, 1.0 equiv) and the mixture was stirred at room temperature for 5 h[26]. Then 2 M HCl was added to the mixture to adjust the PH to 3.0 and the CH_3OH solvent was removed under reduced pressure. The crude product was diluted with water (50 mL) and extracted with EtOAc (50 mL × 2), the combined organic layers dried with Na_2SO_4, filtered, and concentrated under reduced pressure. The residual mixture was purified via silica gel column chromatography (CH_2Cl_2/CH_3OH, 25/1, v/v) to afford target compound **A1** (0.92 g, 52% yield) as a white solid. ^{1}H NMR (600 MHz, CD_3OD) δ 8.32 (s, 1H), 7.72 (s, 1H), 7.48-7.41 (m, 1H), 7.16 (d, J = 8.6 Hz, 2H), 6.92-6.87 (m, 1H), 6.85-6.80 (m, 3H), 4.66 (d, J = 14.4 Hz, 1H), 4.57 (d, J = 14.3 Hz, 1H), 3.96 (t, J = 6.2 Hz, 2H), 3.38 (d, J = 2.3 Hz, 2H), 2.96 (dd, J = 13.8, 1.2 Hz, 1H), 2.77 (d, J = 13.8 Hz, 1H), 2.502.41 (m, 4H), 2.35 (bs, 4H), 2.27 (t, J = 7.4 Hz, 2H), 2.07-2.02 (m, 2H). ^{13}C NMR (151 MHz, CD_3OD) δ 170.59, 162.39 (dd, J = 247.7, 12.2 Hz), 158.93 (dd, J = 246.5, 12.2 Hz), 158.52, 149.38, 144.30, 130.72, 129.13 (d, J = 8.7 Hz), 126.22, 125.24 (d, J = 10.5 Hz), 113.78, 110.26 (d, J = 21.0 Hz), 103.11 (t, J = 26.9 Hz), 73.51 (d, J = 4.9 Hz), 66.29, 62.51, 60.83, 55.65, 52.73, 51.76, 28.54, 24.65.

Target compounds **A2-A13** were synthesized according to the synthetic method of target compound **A1**.

4.1.2. 8-(4-((4-(2-(2,4-difluorophenyl)-2-hydroxy-3-(1H-1,2,4-triazol-1yl)propyl)piperazin-1-yl)methyl)phenoxy)-N-hydroxyoctanamide (**A5**)

White solid, 55% yield. ^{1}H NMR (600 MHz, CD_3OD) δ 8.34 (s, 1H), 7.75 (s, 1H), 7.46 (dd, J = 6.7 Hz, 1H), 7.17 (d, J = 8.5 Hz, 2H), 6.96-6.87 (m, 1H), 6.85-6.81 (m, 3H), 4.67 (d, J = 14.3 Hz, 1H), 4.59 (d, J = 14.3 Hz, 1H), 3.93 (t, J = 6.4 Hz, 2H), 3.43-3.37 (m, 2H), 2.98 (d, J = 13.8 Hz, 1H), 2.78 (d, J = 13.8 Hz, 1H), 2.47 (bs, 4H), 2.37 (bs, 4H), 2.10 (t, J = 7.4 Hz, 2H), 1.78-1.71 (m, 2H), 1.67-1.59 (m, 2H), 1.50-1.42 (m, 2H), 1.42-1.31 (m, 4H). ^{13}C NMR (151 MHz, CD_3OD) δ 171.54, 162.70 (dd, J = 247.8, 12.2 Hz), 159.28 (dd, J = 246.7, 11.9 Hz), 158.59, 149.73, 144.67, 130.62, 129.43 (d, J = 14.8 Hz), 128.32, 125.83 (d, J = 9.9 Hz), 113.91, 110.65 (d, J = 20.9 Hz), 103.52 (t, J = 26.8 Hz), 73.50 (d, J = 5.2 Hz), 67.56, 63.03, 61.78, 56.13 (d, J = 4.2 Hz), 53.84, 52.46, 32.39, 28.93, 28.69, 25.61, 25.29. HRMS (ESI) *m/z*: calcd for $C_{30}H_{40}F_2N_6O_4$ $[M + H]^+$, 587.3157; found 587.3156. HPLC purity: 96.4%.

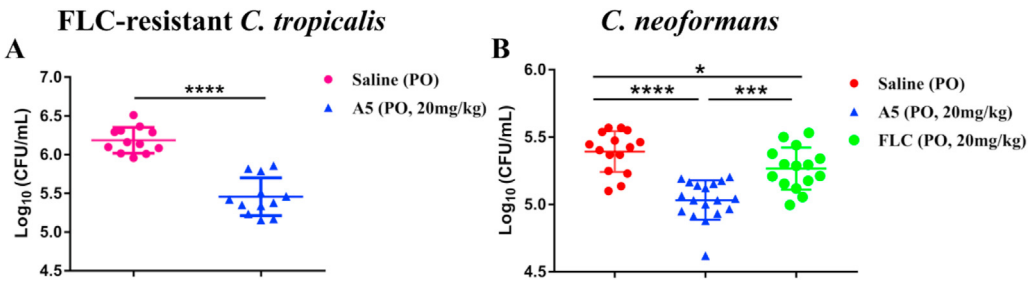

Fig. 7. *In vivo* antifungal activity of compound **A5**. (A) *C. tropicalis* 5008 mouse model; (B) *C. neoformans* H99 mouse model. Cyclophosphamide was injected intraperitoneally 24 h before the fungal infection in order to destroy the immune system. The experiment was divided into 3 groups: saline group, compound **A5** oral (PO) administration group (20 mg/kg) and FLC oral (PO) administration group (20 mg/kg). *$P < 0.05$, **$P < 0.01$, ***$P < 0.001$, ****$P < 0.0001$, determined by Student's *t*-test.

*4.1.3. 2-(4-((5-(4-(2-(2,4-difluorophenyl)-2-hydroxy-3-(1H-1,2,4-triazol-1-yl)propyl) piperazin-1-yl)pentyl)oxy)phenyl)-N-hydroxyacetamide (**A7**)*

White solid, 51% yield. ^{1}H NMR (600 MHz, CD_3OD) δ 8.33 (s, 1H), 7.74 (s, 1H), 7.49-7.42 (m, 1H), 7.17 (d, J = 8.6 Hz, 2H), 6.93-6.89 (m, 1H), 6.85-6.79 (m, 3H), 4.67 (d, J = 14.3 Hz, 1H), 4.59 (d, J = 14.3 Hz, 1H), 3.92 (t, J = 6.3 Hz, 2H), 3.30 (s, 2H), 2.98 (d, J = 13.8, 1.1 Hz, 1H), 2.78 (d, J = 13.8 Hz, 1H), 2.47 (bs, 4H), 2.38 (bs, 4H), 2.32-2.28 (m, 2H), 1.78-1.72 (m, 2H), 1.55-1.49 (m, 2H), 1.47-1.41 (m, 2H). ^{13}C NMR (151 MHz, CD_3OD) δ 169.80, 162.81 (dd, J = 247.9, 12.3 Hz), 161.74, 159.29 (dd, J = 246.6, 12.0 Hz), 158.09, 149.90, 144.71, 129.69, 127.09, 125.03 (d, J = 12.8 Hz), 114.21, 110.76 (d, J = 20.9 Hz), 103.56 (t, J = 27.0 Hz), 74.90 (d, J = 5.0 Hz), 67.12 (d, J = 10.1 Hz), 62.49, 56.44, 55.79, 51.81, 51.04, 38.32, 28.31, 23.29, 22.88. HRMS (ESI) *m/z*: calcd for $C_{28}H_{36}F_2N_6O_4$ $[M + H]^+$, 559.2844; found 559.2852.

*4.1.4. 7-(4-(4-((4-(2-(2,4-difluorophenyl)-2-hydroxy-3-(1H-1,2,4-triazol-1-yl)propyl)piperazin-1-yl)methyl)phenyl)-5-oxo-4,5-dihydro-1H-1,2,4-triazol-1-yl)-N-hydroxyheptanamide (**A12**)*

White solid, 53% yield. ^{1}H NMR (600 MHz, CD_3OD) δ 8.32 (s, 1H), 8.13 (s, 1H), 7.73 (s, 1H), 7.54 (d, J = 8.3 Hz, 2H), 7.47-7.42 (m, 3H), 6.92-6.88 (m, 1H), 6.84-6.80 (m, 1H), 4.66 (d, J = 14.3 Hz, 1H), 4.58 (d, J = 14.3 Hz, 1H), 3.82 (t, J = 6.9 Hz, 2H), 3.50 (s, 2H), 2.98 (d, 1H), 2.77 (d, J = 13.8 Hz, 1H), 2.46 (m, 4H), 2.38 (bs, 4H), 2.08 (t, J = 7.3 Hz, 2H), 1.80-1.75 (m, 2H), 1.64-1.58 (m, 2H), 1.38-1.35 (m, 4H). ^{13}C NMR (151 MHz, CD_3OD) δ 171.37, 162.74 (dd, J = 247.6, 12.3 Hz), 159.31 (dd, J = 246.5, 11.8 Hz), 152.21, 149.72, 144.69, 137.03, 134.84, 132.93, 130.34, 129.47 (d, J = 6.1 Hz), 125.82 (d, J = 9.7 Hz), 122.05, 110.63 (d, J = 21.0 Hz), 103.49 (t, J = 26.8 Hz), 73.55 (d, J = 5.3 Hz), 63.06, 61.63, 56.12, 53.98, 52.61, 45.01, 28.14, 27.99, 25.74, 25.19. HPLC purity: 96.6%.

4.2. Biological activity

4.2.1. MIC_{80} determination

The antifungal activity of the target compounds *in vitro* was determined by plate microdilution method according to CLSI (M27A3). Experiment was performed on the 96-well plated and fungal cells (1×10^3 cells per well) in RMPI 1640 medium, the test compounds were added in two-fold serial dilutions at 35 °C for 48 h (*C. tropicalis*) or 72 h (*C. neoformans*). Then the optical density OD at 630 nm (OD_{630}) was monitored to evaluate the growth of fungi and calculate the inhibition rate of each well. The minimum concentration with inhibition over 80% of each compound was used as MIC_{80}.

4.2.2. Time-growth curve assay

The assay was performed according to our previously reported method [49]. Exponentially growing *C. tropicalis* 5008 cells and *C. neoformans* H99 cells were incubated into YEPD medium, collected and resuspended in 3 mL of fresh RPMI 1640 medium with a concentration of 1×10^5 cells/mL, 1×10^6 cells/mL respectively. FLC and compound **A5** at different concentrations were added to treat the fungal cells with constant shaking cultured (240 rpm/min) at 30 °C, then the numbers of the fungal cells at the specified times (0, 6, 12, 24, 36, 48 h) were measured via OD_{630}. The experiment was conducted triply.

4.2.3. In vitro biofilm formation assay

According to the previously reported protocols [50], the biofilm formation assay of compound **A5** and FLC against the FLC-resistant *C. tropicalis* 5008 and *C. neoformans* H99 were performed. The fungal cells suspensions were prepared from the exponential growth stage of *C. tropicalis* 5008 or *C. neoformans* H99 cells in YEPD medium and diluted with RPMI 1640 medium to 1×10^6 CFU/mL, respectively. Then the fungal cells suspensions were added to a 96-well plate and incubated at 37 °C for 1.5 h. After that, the upper RPMI 1640 medium liquid of each well was absorbed and removed, and washed with 100 μL PBS to remove the nonadherent fungal cells. Compound **A5** was added at different concentrations with FLC as positive control, and the plate was incubated in at 37 °C for 24 h. Finally, a semiquantitative determination of biofilm formation was performed using the XTT reduction method.

4.2.4. In vitro hyphal formation assay

The exponential growth stage of *C. tropicalis* 5008 cells in YEPD medium and diluted with 1.5 mL spider medium to 1×10^5 CFU/mL. The fungal cells suspension was added to a 12-well plate, and compound **A5** was added at different concentrations with FLC as positive drug. After the fungal cell incubation at 37 °C for 7 h, the difference in morphology between drug-treated group and no drug group were recorded on the live cell imaging inverted microscope.

4.2.5. In vitro capsule formation assay

The capsule formation assay was performed according to previously reported methods with a few optimizations [51]. Exponentially growing *C. neoformans* H99 cells were incubated into YEPD medium, collected and resuspended in 2 mL of PBS at a concentration of 1×10^7 cells/mL. Then the 100 μL fungal cells suspension was added into a 12-well culture plate, 200 μL FBS and 1.7 mL DMEM were added in each well with different concentrations of compound **A5**, no drug treated group as black control. The 12-well culture plate was placed in 37 °C with 10% CO_2 atmosphere for 24 h. For capsule imaging, 100 μl of fungal cells suspension was mixed with 10 μL India Ink (Kingmorn, Shanghai) and observed under Laser scanning Confocal Microscopy at a magnification of 63× (Leica SP5, Germany). The 10 different fields were randomly chosen to photographed. For the calculation of capsule size, the diameter of whole fungal cell and the diameter of fungal cell body were measured by using ImageJ software.

4.2.6. Analysis of fungal sterol composition assay

After treated with compound **A5** with different concentrations in YEPD medium, the *C. tropicalis* 5008 and *C. neoformans* H99 cells were collected (wet weight about 1.0 g). Then the mixtures were mixed with 10 mL saponifier (90% ethanol solution containing 15% NaOH) at 80 °C for 1 h. After that, 10 mL of petroleum ether (boiling range: 30–60 °C) was added to extract the sterols of each groups for 3 times. The extracted solutions were evaporated under reduced pressure, and 1 mL cyclohexane was added to dissolve the residue. Finally, the sterols composition of each compound group was analyzed by using GC-MS, and the identification of sterols was achieved by using the molecular fragments in each peak of GC-MS chromatograms to match the corresponding sterol compound in the NIST (the National Institute of Standards and Technology) reference database.

4.2.7. Whole fungal cell HDACs enzymatic assay

Referring to the previously reported fungal HDAC enzymatic method and with a few modifications[26]. The exponential growth phase of *C. tropicalis* 5008 and *C. neoformans* H99 cells were collected with the wet weight at 100 mg. Then they were treated by snailase (3 mg) and 2-mercapto-ethanol (12 μL) in the snailase reaction buffer (3 mL) to prepare fungal protoplast. The protoplast was dispersed in PBS (20 mL) and added into 96 well plate with 100 μL per well. Then the different concentrations of compounds were added to and further incubated at 35 °C for 12 h. The HDAC substrate Boc-Lys(Ac)-AMC was added and adjusted the substrate concentration to 30 μM in each well, then the plate incubated at 37 °C for 6 h. Subsequently, 100 μL of HDAC enzymatic assay stop solution were added and incubated at 37 °C for 2 h. Finally, 100 μL culture of each well was added to 96-well plate to monitor the fluorescence intensity (Ex = 360 nm, Em = 460 nm), which was used to calculate the HDAC inhibition rate.

4.2.8. RT-qPCR analysis

Exponentially growing *C. tropicalis* 5008 cells were used to inoculate in 10 mL YPD with different concentrations of compound **A5** and DMSO as a blank control. After the cultures were incubated at 35 °C for 24 h, Total RNA of each group was isolated according to the manufacture's protocol (Column Fungal RNAOUT, TIANDZ, China), then the RNA was converted to cDNA by a reverse transcription kit (TaKaRa, Biotechnology). Quantitative real-time RT-PCR analysis were performed by using the StepOne System Fast real-time PCR system (Applied Biosystems) with *ACT1* was used as an internal control gene. The relative fold change of the gene expression levels for each group was calculated using formula $2^{(-\Delta\Delta CT)}$. Real-time PCR reaction for each cDNA was performed in triplicate. The Gene-specific primers used in the assay are shown in Table S1.

The *C. neoformans* H99 cells RNA isolation was different from *C. tropicalis* 5008 cells. Initially, exponentially growing *C. neoformans* H99 cells were used to inoculate in 50 mL YPD with different concentrations of compound **A5**. After incubated at 35 °C for 24 h, the cultures grind thoroughly in liquid nitrogen for using. Total RNA of each group was isolated according to the manufacture's protocol (RNeasy Plant Mini kit, QIAGEN), the RNA reverse transcription and RT-PCR analysis were similar to *C. tropicalis.* The Gene-specific primers used in the assay are shown in Table S1.

4.2.9. In vivo antifungal assay

Female ICR mice (weight: 18–20 g, age: 4–6 weeks) were used to build the *in vivo* experimental model, which purchased from Shanghai Experimental Animal Center, Chinese Academy of Sciences. The invasive *C. tropicalis* infective mice model was established by intraperitoneally injected cyclophosphamide (100 mg/kg) 24 h in advance and intravenously injected 1×10^5 CFU *C. tropicalis* 5008 cells on day 0. The murine model of CM was established by intravenously injected 2×10^5 CFU *C. neoformans* H99 cells on day 0. Compound **A5** (20 mg/kg) and FLC (20 mg/kg) were given orally once a day at regular time, and the mice were administered with drug solutions for 5 consecutive days with saline as blank control. On day 6, the mice were euthanized, then kidney for *C. tropicalis* infective mice and brain for *C. neoformans* infective mice were picked aseptically. The picked infective organ was homogenized and the homogenates in appropriate concentration were inoculated to Sabouraud's Dextrose Agar (SDA) medium at 35 °C for 48 h. Finally, counted the number of single colonies on each SDA medium, and further calculated the fungal burden of the kidney tissue or brain tissue. ANOVA was used to analyze the differences among the groups.

Declaration of competing interest

The authors declare that they have no known competing financial interests or personal relationships that could have appeared to influence the work reported in this paper.

Acknowledgment

This work was supported by the National Natural Science Foundation of China (Grant 81725020 to C.S. and 81973175 to N.L.), the Innovation Program of Shanghai Municipal Education Commission (Grant 2019-01-07-00-07-E00073 to C.S.), and the Science and Technology Commission of Shanghai Municipality (Grant 20S11900400 to C.S.).

Appendix A. Supplementary data

Supplementary data to this article can be found online at https://doi.org/10.1016/j.ejmech.2021.113524.

References

[1] G.D. Brown, D.W. Denning, S.M. Levitz, Tackling human fungal infections, Science 336 (2012) 647.
[2] M.C. Fisher, N.J. Hawkins, D. Sanglard, S.J. Gurr, Worldwide emergence of resistance to antifungal drugs challenges human health and food security, Science 360 (2018) 739–742.
[3] L.Y. Chai, D.W. Denning, P. Warn, Candida tropicalis in human disease, Crit. Rev. Microbiol. 36 (2010) 282–298.
[4] M. Negri, S. Silva, M. Henriques, R. Oliveira, Insights into Candida tropicalis nosocomial infections and virulence factors, Eur. J. Clin. Microbiol. Infect. Dis. 31 (2012) 1399–1412.
[5] H. Xin, Effects of immune suppression in murine models of disseminated Candida glabrata and Candida tropicalis infection and utility of a synthetic peptide vaccine, Med. Mycol. 57 (2019) 745–756.
[6] C.C. Lai, C.K. Tan, Y.T. Huang, P.L. Shao, P.R. Hsueh, Current challenges in the management of invasive fungal infections, J. Infect. Chemother. 14 (2008) 77–85.
[7] R. Rajasingham, R.M. Smith, B.J. Park, J.N. Jarvis, N.P. Govender, T.M. Chiller, D.W. Denning, A. Loyse, D.R. Boulware, Global burden of disease of HIV-associated cryptococcal meningitis: an updated analysis, Lancet, Inf. Disp. 17 (2017) 873–881.
[8] F.L. Mayer, J.W. Kronstad, Disarming fungal pathogens: Bacillus safensis inhibits virulence factor production and biofilm formation by Cryptococcus neoformans and Candida albicans, mBio 8 (2017) e01517.
[9] F.C. Odds, Genomics, molecular targets and the discovery of antifungal drugs, Rev. Iberoam. Micol. 22 (2005) 229–237.
[10] F.C. Odds, A.J. Brown, N.A. Gow, Antifungal agents: mechanisms of action, Trends Microbiol. 11 (2003) 272–279.
[11] J. Kim, J.E. Lee, J.S. Lee, Histone deacetylase-mediated morphological transition in Candida albicans, J. Microbiol. 53 (2015) 805–811.
[12] L. Cui, J. Miao, T. Furuya, Q. Fan, X. Li, P.K. Rathod, X.Z. Su, L. Cui, Histone acetyltransferase inhibitor anacardic acid causes changes in global gene expression during in vitro Plasmodium falciparum development, Eukaryot. Cell 7 (2008) 1200–1210.
[13] I. Lee, J.H. Oh, E.K. Shwab, T.R. Dagenais, D. Andes, N.P. Keller, HdaA, a class 2 histone deacetylase of Aspergillus fumigatus, affects germination and

secondary metabolite production, Fungal Genet. Biol. 46 (2009) 782–790.
[14] M.B. Lohse, A.D. Johnson, Temporal anatomy of an epigenetic switch in cell programming: the white-opaque transition of C. albicans, Mol. Microbiol. 78 (2010) 331–343.
[15] D. Hnisz, T. Schwarzmuller, K. Kuchler, Transcriptional loops meet chromatin: a dual-layer network controls white-opaque switching in Candida albicans, Mol. Microbiol. 74 (2009) 1–15.
[16] N. Robbins, M.D. Leach, L.E. Cowen, Lysine deacetylases Hda1 and Rpd3 regulate Hsp90 function thereby governing fungal drug resistance, Cell Rep. 2 (2012) 878–888.
[17] O.W. Liu, C.D. Chun, E.D. Chow, C. Chen, H.D. Madhani, S.M. Noble, Systematic genetic analysis of virulence in the human fungal pathogen Cryptococcus neoformans, Cell 135 (2008) 174–188.
[18] P.A. Dumesic, C.M. Homer, J.J. Moresco, L.R. Pack, E.K. Shanle, S.M. Coyle, B.D. Strahl, D.G. Fujimori, J.R. Yates 3rd, H.D. Madhani, Product binding enforces the genomic specificity of a yeast polycomb repressive complex, Cell 160 (2015) 204–218.
[19] L. Kmetzsch, Histone deacetylases: targets for antifungal drug development, Virulence 6 (2015) 535–536.
[20] S. Su, X. Li, X. Yang, Y. Li, X. Chen, S. Sun, S. Jia, Histone acetylation/deacetylation in Candida albicans and their potential as antifungal targets, Future Microbiol. 15 (2020) 1075–1090.
[21] M.A. Pfaller, S.A. Messer, N. Georgopapadakou, L.A. Martell, J.M. Besterman, D.J. Diekema, Activity of MGCD290, a Hos2 histone deacetylase inhibitor, in combination with azole antifungals against opportunistic fungal pathogens, J. Clin. Microbiol. 47 (2009) 3797–3804.
[22] W.L. Smith, T.D. Edlind, Histone deacetylase inhibitors enhance Candida albicans sensitivity to azoles and related antifungals: correlation with reduction in CDR and ERG upregulation, Antimicrob. Agents Chemother. 46 (2002) 3532–3539.
[23] A. Mai, D. Rotili, S. Massa, G. Brosch, G. Simonetti, C. Passariello, A.T. Palamara, Discovery of uracil-based histone deacetylase inhibitors able to reduce acquired antifungal resistance and trailing growth in Candida albicans, Bioorg. Med. Chem. Lett 17 (2007) 1221–1225.
[24] A. Anighoro, J. Bajorath, G. Rastelli, Polypharmacology: challenges and opportunities in drug discovery, J. Med. Chem. 57 (2014) 7874–7887.
[25] Y. Huang, G. Dong, H. Li, N. Liu, W. Zhang, C. Sheng, Discovery of janus kinase 2 (JAK2) and histone deacetylase (HDAC) dual inhibitors as a novel strategy for the combinational treatment of leukemia and invasive fungal infections, J. Med. Chem. 61 (2018) 6056–6074.
[26] G. Han, N. Liu, C. Li, J. Tu, Z. Li, C. Sheng, Discovery of novel fungal lanosterol 14alpha-demethylase (CYP51)/histone deacetylase dual inhibitors to treat azole-resistant candidiasis, J. Med. Chem. 63 (2020) 5341–5359.
[27] Z. Jiang, Y. Wang, W. Wang, S. Wang, B. Xu, G. Fan, G. Dong, Y. Liu, J. Yao, Z. Miao, W. Zhang, C. Sheng, Discovery of highly potent triazole antifungal derivatives by heterocycle-benzene bioisosteric replacement, Eur. J. Med. Chem. 64 (2013) 16–22.
[28] S. Silva, M. Negri, M. Henriques, R. Oliveira, D.W. Williams, J. Azeredo, Candida glabrata, Candida parapsilosis and Candida tropicalis: biology, epidemiology, pathogenicity and antifungal resistance, FEMS Microbiol. Rev. 36 (2012) 288–305.
[29] K. Diba, K. Makhdoomi, E. Nasri, A. Vaezi, J. Javidnia, D.J. Gharabagh, N.H. Jazani, A. Reza Chavshin, P. Badiee, H. Badali, H. Fakhim, Emerging Candida species isolated from renal transplant recipients: species distribution and susceptibility profiles, Microb. Pathog. 125 (2018) 240–245.
[30] S.M. Noble, B.A. Gianetti, J.N. Witchley, Candida albicans cell-type switching and functional plasticity in the mammalian host, Nat. Rev. Microbiol. 15 (2017) 96–108.
[31] S.M. Noble, S. French, L.A. Kohn, V. Chen, A.D. Johnson, Systematic screens of a Candida albicans homozygous deletion library decouple morphogenetic switching and pathogenicity, Nat. Genet. 42 (2010) 590–598.
[32] J.A. Romo, C.G. Pierce, A.K. Chaturvedi, A.L. Lazzell, S.F. Mchardy, S.P. Saville, J.L. Lopez-Ribot, J. Heitman, Development of anti-virulence approaches for candidiasis via a novel series of small-molecule inhibitors of Candida albicans filamentation, mBio 8 (2017) e01991.
[33] J.A. Romo, C.G. Pierce, M. Esqueda, C.Y. Hung, S.P. Saville, J.L. Lopez-Ribot, In vitro characterization of a biaryl amide anti-virulence compound targeting Candida albicans filamentation and biofilm formation, Front. Cell Infect. Microbiol. 8 (2018) 227.
[34] N. Liu, H. Zhong, J. Tu, Z. Jiang, Y. Jiang, Y. Jiang, Y. Jiang, J. Li, W. Zhang, Y. Wang, C. Sheng, Discovery of simplified sampangine derivatives as novel fungal biofilm inhibitors, Eur. J. Med. Chem. 143 (2018) 1510–1523.
[35] R.M. Donlan, J.W. Costerton, Biofilms: survival mechanisms of clinically relevant microorganisms, Clin. Microbiol. Rev. 15 (2002) 167–193.
[36] D.D. Li, L.X. Zhao, E. Mylonakis, G.H. Hu, Y. Zou, T.K. Huang, L. Yan, Y. Wang, Y.Y. Jiang, In vitro and in vivo activities of pterostilbene against Candida albicans biofilms, Antimicrob. Agents Chemother. 58 (2014) 2344–2355.
[37] S. Wu, Y. Wang, N. Liu, G. Dong, C. Sheng, Tackling fungal resistance by biofilm inhibitors, J. Med. Chem. 60 (2017) 2193–2211.
[38] T.R. O'Meara, J.A. Alspaugh, The Cryptococcus neoformans capsule: a sword and a shield, Clin. Microbiol. Rev. 25 (2012) 387–408.
[39] A. Casadevall, C. Coelho, R.J.B. Cordero, Q. Dragotakes, E. Jung, R. Vij, M.P. Wear, The capsule of Cryptococcus neoformans, Virulence 10 (2019) 822–831.
[40] K. Okabayashi, R. Kano, S. Watanabe, A. Hasegawa, Expression of capsule-associated genes of Cryptococcus neoformans, Mycopathologia 160 (2005) 1–7.
[41] F. Abe, K. Usui, T. Hiraki, Fluconazole modulates membrane rigidity, heterogeneity, and water penetration into the plasma membrane in Saccharomyces cerevisiae, Biochemistry 48 (2009) 8494–8504.
[42] J.R. Perfect, The antifungal pipeline: a reality check, Nat. Rev. Drug Discov. 16 (2017) 603–616.
[43] N. Robbins, G.D. Wright, L.E. Cowen, Antifungal drugs: the current armamentarium and development of new agents, Microbiol. Spectr. 4 (2016) 1–20.
[44] Y. Lee, E. Puumala, N. Robbins, L.E. Cowen, Antifungal drug resistance: molecular mechanisms in Candida albicans and beyond, Chem. Rev. (2020), https://doi.org/10.1021/acs.chemrev.0c00199.
[45] S. Schubert, P.D. Rogers, J. Morschhauser, Gain-of-function mutations in the transcription factor MRR1 are responsible for overexpression of the MDR1 efflux pump in fluconazole-resistant Candida dubliniensis strains, Antimicrob. Agents Chemother. 52 (2008) 4274–4280.
[46] C. Jiang, D. Dong, B. Yu, G. Cai, X. Wang, Y. Ji, Y. Peng, Mechanisms of azole resistance in 52 clinical isolates of Candida tropicalis in China, J. Antimicrob. Chemother. 68 (2013) 778–785.
[47] T. Noel, The cellular and molecular defense mechanisms of the Candida yeasts against azole antifungal drugs, J. Mycol. Med. 22 (2012) 173–178.
[48] F. Brandao, S.K. Esher, K.S. Ost, K. Pianalto, C.B. Nichols, L. Fernandes, A.L. Bocca, M.J. Pocas-Fonseca, J.A. Alspaugh, HDAC genes play distinct and redundant roles in Cryptococcus neoformans virulence, Sci. Rep. 8 (2018) 5209.
[49] S. Wang, Y. Wang, W. Liu, N. Liu, Y. Zhang, G. Dong, Y. Liu, Z. Li, X. He, Z. Miao, J. Yao, J. Li, W. Zhang, C. Sheng, Novel carboline derivatives as potent antifungal lead compounds: design, synthesis, and biological evaluation, ACS Med. Chem. Lett. 5 (2014) 506–511.
[50] Z. Jiang, N. Liu, D. Hu, G. Dong, Z. Miao, J. Yao, H. He, Y. Jiang, W. Zhang, Y. Wang, C. Sheng, The discovery of novel antifungal scaffolds by structural simplification of the natural product sampangine, Chem. Commun. 51 (2015) 14648–14651.
[51] F.A. Brandao, L.S. Derengowski, P. Albuquerque, A.M. Nicola, I. Silva-Pereira, M.J. Pocas-Fonseca, Histone deacetylases inhibitors effects on Cryptococcus neoformans major virulence phenotypes, Virulence 6 (2015) 618–630.